Friction versus texture at the approach of a granular avalanche

Lydie Staron[1] and Farhang Radjai[2]
[1]*Department of Applied Mathematics and Theoretical Physics, University of Cambridge, Wilberforce Road, Cambridge CB3 0WA, United Kingdom*
[2]*Laboratoire de Mécanique et Génie Civil, CNRS-Université Montpellier II, Place Eugène Bataillon, F-34095 Montpellier Cx, France*
(Received 14 April 2005; published 27 October 2005)

We perform an analysis of the granular texture of a granular bed close to stability limit. Our analysis is based on a unique criterion of friction mobilization in a simulated two-dimensional packing. In this way, we recover the bimodal character of granular texture and the coexistence of weak and strong phases in the sense of distinct contacts populations. Moreover, we show the existence of a well-defined subset of contacts within the weak contact network. These contacts are characterized by their important friction and form a highly coherent population in terms of fabric. They play an antagonistic role with respect to force chains. Thus, we are able to discriminate between incoherent contacts and coherent contacts in the weak phase and to specify the role that the latter plays in the destabilization process.

DOI: 10.1103/PhysRevE.72.041308 PACS number(s): 45.70.Ht, 45.70.Cc

Disordered systems exhibit critical behaviors which often result in the emergence of rare "catastrophic" events for which predictive modeling is problematic [1]. Earthquakes, and more generally, rupture of composite materials, are well-known examples of this criticality [2,3]. Dry cohesionless granular matter, characterized by a generic disorder induced by the rigidity of the grains and the highly dissipative contacts between them, obeys the same type of behavior. Its response to loading involves a succession of microplastic events which eventually lead to a catastrophic failure [4,5], for instance, a surface avalanche.

In spite of their intrinsic disorder, granular materials obey a well-defined organization commonly referred to as *granular texture* [6]. Related to force transmission, the granular texture relies on a discrimination between intergrains contacts, depending on the intensity of the force they transmit regarding the average force. It was shown that contacts transmitting a force larger than the average force exhibit, in the mean, different mechanical properties than the rest of the contacts [7]. In particular, this fraction of the contacts contributes to the quasitotality of the shear stress. Known as the *strong contact network* and forming *force chains*, it has been extensively studied on the grounds that it is responsible for the mechanical strength of the whole granular structure [8–11]. By contrast, weak forces merely result in a mean pressure and only marginally contribute to the stress state. As a result, it is tempting to attribute the properties of a granular pile, in particular at stability limit, to the strong contact network only.

Another fundamental aspect of granular packings behavior is the intergrain friction [12,13]. Frictional contacts form the dissipative part of the contact network and are essential for the identification of precursors of the destabilization [14–16]. Yet the organization of frictional contacts, and its relation with the organization of the stress-induced texture, has attracted less attention. While force chains are held responsible for the stability of granular packing, ensuring its mechanical strength, frictional contacts result in local instabilities and constitute a threat to stability. Understanding the interplay between texture and friction is a key question in the perspective of understanding the transition of a static granular slope to failure [17,18].

In this contribution, we study the organization of friction forces in a simulated granular slope close to the stability limit. We propose an analysis of granular texture based solely on the criterion of friction mobilization. Doing so, we are able to recover the biphasic nature of the granular texture as described in Ref. [7]. More importantly, we show the existence of a well-defined population of contacts, highly frictional and coherent in the sense that their orientation results in a well-defined mean direction due to their anisotropy, and coexisting in the weak phase with a large population of incoherent contacts. In other words, the weak phase is hosting a coherent class of contacts whose role is essential in the evolution toward avalanching in spite of its poor contribution to the mechanical quantities one can measure in a granular packing. These findings enable us to revisit the characteristics of the granular texture and the respective roles of the weak and the strong contacts in the destabilization process.

This analysis was performed by means of two-dimensional numerical simulation. We have used a contact dynamics algorithm [19] assuming perfectly rigid grains interacting at contacts through a hard core repulsion and a Coulomb friction law. Beyond the fact that contact dynamics treats them as strictly nonsmooth, these contact laws do not differ from those more commonly used in discrete simulations. We consider a granular bed built by random rain of 8000 circular grains of diameters varying in a ratio 1.5 to induce geometrical disorder. The solid fraction of the packing is 0.82. The height of the bed is $40D$ and its width is $200D$, where D is the grain mean diameter. To prevent rigid boundary effects, the bed is periodic in the horizontal direction, namely no vertical walls are introduced to confine the packing. A constant rotation rate is applied (corresponding to a rotation of 10^{-3}deg per time step), gradually bringing the slope θ of the bed from initially zero to the limit value θ_c for which a surface avalanche is triggered.

The Coulomb friction law imposes an upper limit on the tangential force f_T at contact. This upper limit (the Coulomb threshold) is given by μf_N, where f_N is the normal force at

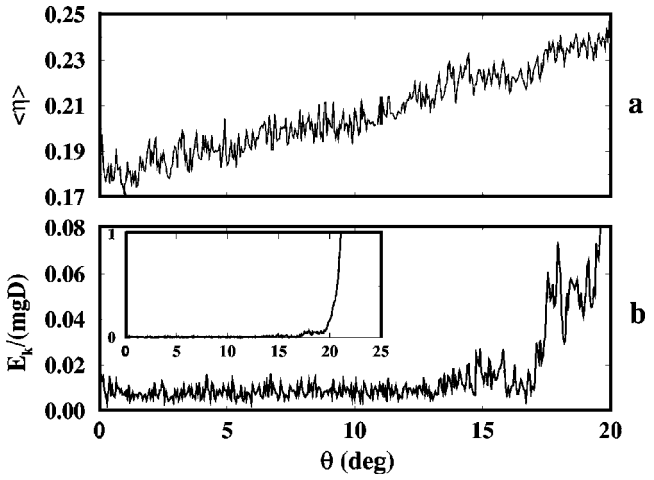

FIG. 1. (a) Mean mobilization of friction forces $\langle \eta \rangle_{N_c}$ averaged over all the contacts and (b) mean kinetic energy E_k normalized by the typical potential energy of a grain of mass m for a height D as a function of the slope angle θ.

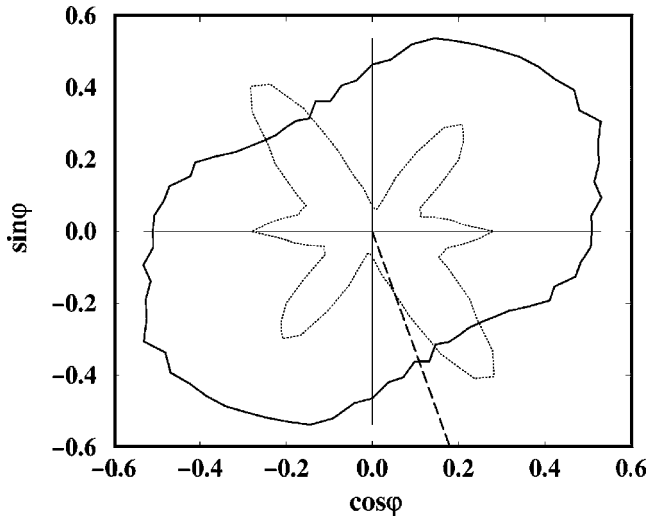

FIG. 2. Polar representation of the mean friction mobilization η_φ (plain line) as a function of the orientation φ of the contacts, and angular map of contact orientations in arbitrary units (dotted lines). The dashed line shows the direction of gravity.

contact and μ is the coefficient of friction. A necessary condition for slip motion to occur at any contact is $f_T = \mu f_N$. In the following, the value of μ is set to 0.5 and its influence, though not investigated here, will be discussed later. A coefficient of restitution allows for the modeling of energy exchanges during binary collisions; since we are interested in microplasticity only, we set its value to zero and consider purely dissipative contact interactions. The mobilization of friction at each contact is simply measured by the ratio of the tangential to the normal force times the coefficient of friction as follows:

$$\eta = \frac{1}{\mu} \frac{f_T}{f_N}, \tag{1}$$

with $\eta \in [0,1]$ following the friction law. The case $\eta = 1$ coincides with the Coulomb threshold and a probable slip motion at the contact. We compute the mean value $\langle \eta \rangle$ over the total number of contacts N_c in the packing as a function of the slope angle θ [Fig. 1(a)]. The mean normalized kinetic energy of the grains as a function of θ is displayed in Fig. 1(b). The onset of the avalanche occurs for $\theta = \theta_c \simeq 20°$. While the mean level of friction increases regularly, we observe some dynamical activity intensifying a few degrees before θ_c. This interval corresponds to a metastable state during which local dynamical rearrangements occur more frequently due to an enhanced mobilization of friction [17,20]. In the following, we thus focus on this interval of slope angles $\Delta_\theta = [\theta_c - 3°, \theta_c]$, and the quantities discussed hereafter are averaged over it.

A picture of the mobilization of friction depending on contact orientation is obtained when plotting the value of η averaged over angular sectors $\varphi + \Delta\varphi$ for contacts directions as follows:

$$\eta_\varphi = \frac{1}{N_c^\varphi} \sum_{\alpha=1}^{N_c^\varphi} \eta^\alpha, \tag{2}$$

where N_c^φ is the number of contacts for which the orientation of the unit vector $\boldsymbol{n}$ normal to the contact plan belongs to $[\varphi, \varphi + \Delta\varphi]$. The function $\eta_\varphi(\varphi)$ is plotted in Fig. 2 in polar coordinates. The slope of the granular bed coincides with the horizontal direction, and the direction of gravity is represented by a dashed line (at $-70°$). We observe a higher mobilization of friction for contacts directed at $\simeq 25°[\pi]$, i.e., nearly perpendicular to the gravity. Note that this angular map of friction mobilization does not compare with the angular map of contact orientations, also shown in Fig. 2.

We consider now different populations of contacts following their friction level η. We introduce a parameter ξ to which the friction level η^α is compared for each contact α. A contact α belongs to C_ξ if $\eta^\alpha \geq (1 - \xi)$,

$$C_\xi = \{\alpha \in N_c / \eta^\alpha \geq (1 - \xi)\}. \tag{3}$$

The parameter ξ varies in the interval [0,1]. The number of contacts belonging to C_ξ is N_ξ. The cumulative proportion $p_\xi = N_\xi / N_c$ of contacts belonging to C_ξ is plotted against ξ in Fig. 3. For ξ close to 0 (i.e., for a high mobilization of friction), p_ξ reaches 18%, exceeding by far the case of a uniform distribution. This value bespeaks the existence of a local peak in the distribution of η (as can be seen in the noncumulative distribution, inset graph in Fig. 3). Contacts such that $\xi \to 0$ thus form a well-defined subset. In the same way, the increase of p_ξ when $\xi \to 1$ is more rapid than a uniform distribution would allow, showing again the nonuniformity of the distribution of friction at contacts. We have checked that these features were robust with respect to μ and the boundary conditions in piles close to stability limit.

To compare the anisotropy of friction mobilization with the anisotropy of the geometrical contact network, we compute *partial fabric tensors* $\bar{\Phi}^\xi$ defined over the contact subsets C_ξ [21],

$$\Phi_{ij}^\xi = \frac{1}{N_\xi} \sum_{\alpha=1}^{N_\xi} n_i^\alpha n_j^\alpha, \tag{4}$$

where $\boldsymbol{n}^\alpha$ is the unit vector of contact α, and i and j refer to coordinates x and y (with x parallel to the free surface). The

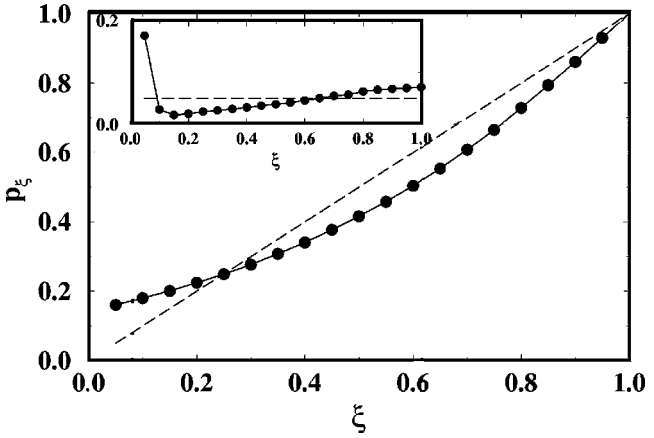

FIG. 3. Proportion of contacts p_ξ belonging to the subset of contacts C_ξ. The dashed line represents the case of a uniform distribution of η. The corresponding noncumulative distribution (namely, the distribution of contacts with $\eta^\alpha = 1-\xi$ instead of $\geqslant 1-\xi$) is shown in the inset graph.

major principal direction θ_Φ^ξ of the tensor $\bar{\Phi}^\xi$ corresponds to the mean direction of the contacts in C_ξ regarding the slope. The difference of the eigenvalues gives the anisotropy a_ξ of the contact subnetwork C_ξ. These two quantities are displayed in Fig. 4 against ξ. We see that the largest anisotropy occurs for $\xi \simeq 0$, i.e., for high friction mobilization. It then declines regularly and passes by its lowest value (close to zero) for $\xi \simeq 0.7$ before increasing again up to $\xi \simeq 1$. This transition coincides with a rotation of $\pi/2$ of the fabric tensor.

Thus, we can discriminate between three groups of contacts on the unique criterion of friction mobilization.

(i) Contacts with a very high mobilization of friction ($\xi \to 0$), i.e., contacts where slip motion is likely to happen. Their orientations obey a maximum anisotropy (0.75), three times superior to the anisotropy of the whole packing and define a mean direction at $\simeq 40°$, orthogonal to the major stress direction ($\simeq -50°$). These contacts are thus forming a

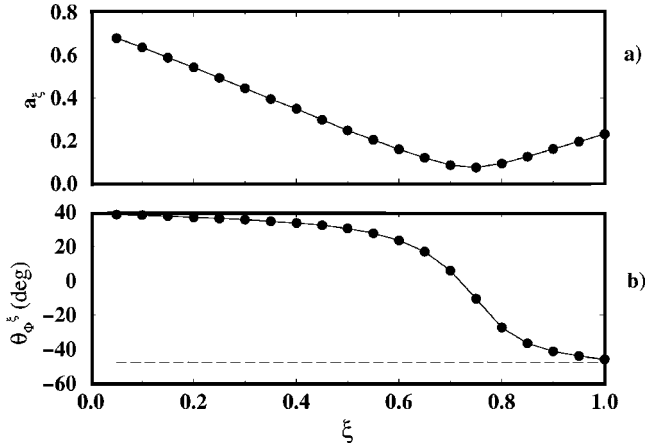

FIG. 4. (a) Anisotropy a_ξ of the contact network in the subset C_ξ and (b) major fabric direction θ_Φ^ξ (counted positively anticlockwise) as a function of ξ (see text). The dashed line shows the major stress direction over all the contacts.

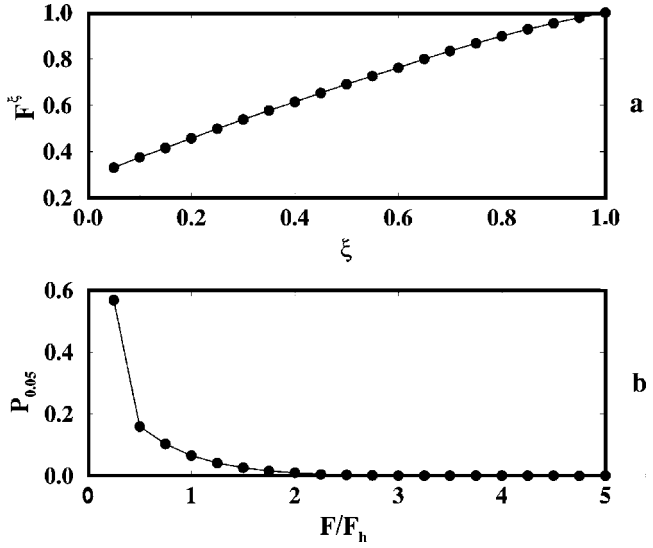

FIG. 5. (a) Mean force F^ξ transmitted by contacts of C_ξ as a function of ξ and (b) probability density function $P_{0.05}$ of F/F_h within the subset of contacts $C_{0.05}$.

highly *coherent* subset in terms of fabric.

(ii) Contact with intermediate level of friction mobilization ($0.1 < \xi < 0.7$): They very weakly contribute to the geometrical anisotropy. Accordingly, their mean orientation allows only for a small deviation from the direction dictated by the first group of contacts. Their small contribution to the fabric suggests that they form an *incoherent* ensemble.

(iii) Contact with a very low mobilization of friction ($\xi \to 1$): They strongly contribute to the geometrical anisotropy. Accordingly, their direction allows for a dramatic rotation of the fabric tensor, forcing the latter to follow the major stress direction. Their strong contribution to the fabric shows that they form a *coherent* ensemble. They represent 40% of the total number of contacts (see Fig. 3).

Discriminating between contacts on the ground of contact friction discloses features strongly reminiscent of the bimodal character of granular texture [7]. The granular texture is characterized when discriminating between contacts on the ground of the intensity of the force they transmit. In the case of our granular bed, the effect of gravity has to be filtered out to distinguish between weak and strong contacts. This is done by normalizing all contact forces F by the mean contact force F_h at the depth h corresponding to the position of the contact. The mean value F^ξ of the normalized force transmitted by the contacts of C_ξ is plotted in Fig. 5(a) as a function of ξ: higher mobilization of friction force (small ξ) coincides with weaker forces and *vice versa*. This concordance between force transmission and friction mobilization implies that the transitions observed in Fig. 4 partly reflect the transition from the weak to the strong contact network.

Focusing on contacts for which the mobilization of friction is the highest, we consider the subset $C_{0.05}$, i.e., the contacts satisfying $\eta \geqslant 0.95$. For these contacts, we plot in Fig. 5(b) the distribution of the intensity $P_{0.05}(F/F_h)$ of the forces they transmit. We observe that most contacts of $C_{0.05}$ transmit very weak forces, such that $F/\langle F \rangle_h \leqslant 0.25$. In any case, 90% of the contacts of $C_{0.05}$ belong to the weak contact

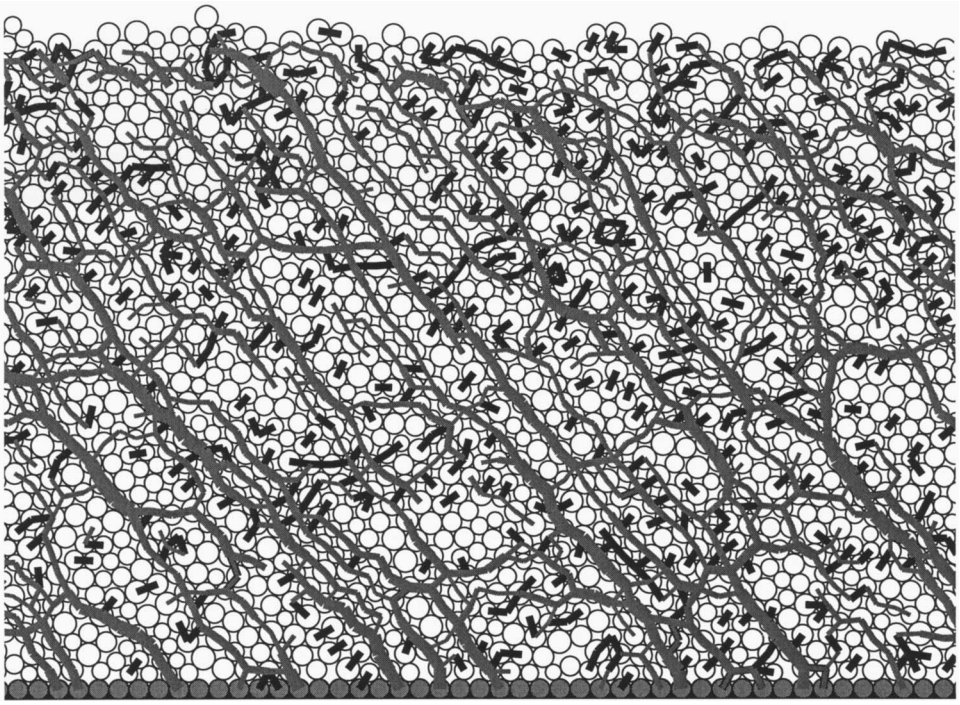

FIG. 6. Sample of the granular bed in the interval $[\theta_c-3°, \theta_c]$. In gray are represented the force chains (contacts such that $F/F_h > 1$) and in black contacts such that $\eta \geqslant 0.95\mu$.

network, namely, those that transmit forces such that $F/F_h < 1$. For comparison, more than 75% of the contacts such that $\eta > 0.7$ transmit strong forces.

The interplay between force transmission and friction mobilization is illustrated in Fig. 6, where one snapshot of the state of the granular pile at an instant of the interval $\Delta_\theta = [\theta_c-3°, \theta_c]$ is shown. In gray are represented the force chains defined by the strong contact network, with linewidth varying proportionally to the force intensity. Black segments of fixed width represent the contacts belonging to $C_{0.05}$. The following features are apparent: contacts of $C_{0.05}$ belong to the weak phase (namely, none of them is part of a force chain), they show a strong geometrical anisotropy (for we distinguish indeed a leading orientation), and their direction is orthogonal to the main stress orientation (i.e., contacts of $C_{0.05}$ are in their great majority transverse to force chains). This organization is also apparent in Fig. 7, where the angular map of contacts [1] orientation is plotted for the totality of the contacts, for the strong phase, for the weak phase excluding the frictional contacts (such as $\eta^\alpha \geqslant 0.95$), and for the frictional contacts.

On the unique criterion of friction mobilization [as defined by Eq. (1)] in a packing close to avalanching, we are able to recover the bimodal character of granular packing and the existence of two distinct phases, in agreement with the analysis in terms of a strong and a weak contact network [7]. Moreover, we show the existence of a well-defined population of contacts within the weak contact network. These contacts are defined by their very high mobilization of friction. They form a highly coherent population, showing a strong anisotropy and a well-defined mean direction. In this sense, they strongly differ from other weak contacts. Their orientation, orthogonal to force chains, and their susceptibility to slip due to their level of friction, impart to them an antagonist role with respect to force chains. Frictional contacts and strong contacts form the extremal state of our analysis, and they play extremal roles in the destabilization process: the latter being sources of stability while the first generate slip motion. All other contacts in the weak network can be assumed to play no role.

This analysis relies on the relative value of the normal and tangential force at contacts and is independent of any mean quantity or any cutoff value reflecting the mean state of the packing. As such, it purely reflects the intrinsic organization of the packing. However, the level of friction mobilization is

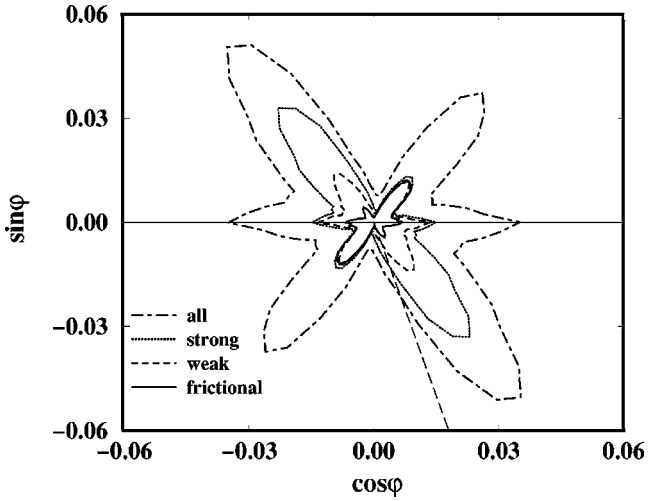

FIG. 7. Angular map of contact orientations φ for all contacts (dashed-dotted line), for strong contacts (dotted line), for weak contacts excluding frictional ones (dashed line), and for frictional contacts (plain line), normalized by the total number of contacts. The long-dashed line shows the direction of gravity.

necessarily measured with respect to the coefficient of friction μ. In particular, the proportion of highly frictional contacts is expected to decrease when the value of μ increases. An investigation of the effect of this parameter on the results reported here should be undertaken. However, in the same way that the characteristics of force transmission are robust with respect to the material properties, we expect the organization of friction to be a robust feature of granular texture.

These results suggest that in a static pile close to avalanching, the relevant description of the granular texture is in terms of the ratio of the tangential component to the normal component of the force transmitted at contacts rather than its simple intensity. Such a description would, in particular, allow further investigation of the correlation lengths emerging in granular system at stability limit based on the mobilization of friction. Recent experiments show that such measurements in real piles could be considered [10]. Here, it should be emphasised that the analysis was performed for a granular pile evolving quasistatically, and no straightforward conclusion can be drawn concerning the organization of forces and friction in a collection of flowing grains.

Back to the description in terms of strong and weak contact networks, the analysis of granular texture in terms of friction allows us to revisit the role of these two entities. The contribution of the strong contact network to the stress state designates it as a solid skeleton of the granular structure and responsible for its stability. By contrast, the weak contact network appears as an "interstitial" phase essentially screened from external loading. In this work, we show that the weak contact network is actually hosting a subset of contacts whose role in destabilization is fundamental. Although forming a less coherent phase when analyzed on the grounds of force transmission (i.e., representing a small anisotropy), the weak contact network contains an intrinsic coherence when analyzed on the grounds of friction. This makes the weak contact network an active agent of the destabilization process. In other words, the macroscopic behavior of the granular packing is partly dependent on a phenomenology which escapes the mean description in terms of stress state.

This work was supported by the Marie Curie European Grant No. 500511.

[1] K. Dahmen and J. P. Sethna, Phys. Rev. B **53**, 14872 (1996).
[2] J. V. Andersen, D. Sornette, and K. Leung, Phys. Rev. Lett. **78**, 2140 (1997).
[3] J. P. Vilotte, J. Schmittbuhl, and S. Roux, in *Nonlinearity and Breakdown in Soft Condensed Matter*, edited by K. Bardham, B. K. Chakrabarti, and A. Hansen (Springer Verlag, Berlin, 1994), p. 54–77.
[4] F. Darve and F. Laouafa, *Numerical Models in Geomaterials* (A. A. Balkema, Publishers, Rotterdam, The Netherlands, 1999), pp.85–90.
[5] D. Volfson, L. S. Tsimring, and I. S. Aranson, Phys. Rev. E **69**, 031302 (2004).
[6] F. Radjai, M. Jean, J. J. Moreau, and S. Roux, Phys. Rev. Lett. **77**, 274 (1996).
[7] F. Radjai, D. E. Wolf, M. Jean, and J. J. Moreau, Phys. Rev. Lett. **80**, 61 (1998).
[8] R. R. Hartley and R. P. Behringer, Nature (London) **421**, 928 (2003).
[9] G. Løvoll, K. J. Måløy, and E. G. Klekkøy, Phys. Rev. E **60**, 5872 (1999).
[10] T. S. Majmudar and R. P. Behringer, Nature (London) **435**, 1079 (2005).
[11] D. M. Mueth, H. M. Jaeger, and S. R. Nagel, Phys. Rev. E **57**, 3164 (1998).
[12] T. Pöschel and V. Buchholtz, Phys. Rev. Lett. **71**, 3963 (1993).
[13] L. E. Silbert, G. S. Grest, and J. W. Landry, Phys. Rev. E **66**, 061303 (2002).
[14] A. Kabla, G. Debregeas, J. M. Di Meglio, and T. Senden, Europhys. Lett. **71**(6), 932 (2005).
[15] S. Nasuno, A. Kudrolli, and J. P. Gollub, Phys. Rev. Lett. **79**, 949 (1997).
[16] L. Staron, J. P. Vilotte, and F. Radjai, Phys. Rev. Lett. **89**, 204302 (2002)
[17] S. Deboeuf, E. M. Bertin, E. Lajeunesse, and O. Dauchot, Eur. Phys. J. B **36**, 105 (2003).
[18] L. Staron, F. Radjai, and J. P. Vilotte, *Powders and Grains 2005* (A. A. Balkema Publishers, Rotterdam, The Netherlands, 2005), pp. 831–835.
[19] M. Jean and J. J. Moreau, in *Proceedings of Contact Mechanics International Symposium* (Presses Polytechniques et Universitaires Romandes, Paris, 1992) pp. 31–48.
[20] A. Daerr and S. Douady, Nature (London) **399**, 241 (1999).
[21] M. Satake, *Proceedings of the IUTAM Symposium on Deformation and Failure of Granular Materials* (A. A. Balkema Publishers, Rotterdam, The Netherlands, 1982).